LETTER

Single-valuedness problem on charge density wave rings

To cite this article: T. Hosokawa *et al* 2015 *EPL* **112** 27005

A LETTERS JOURNAL EXPLORING
THE FRONTIERS OF PHYSICS

October 2015

EPL, **112** (2015) 27005
doi: 10.1209/0295-5075/112/27005

www.epljournal.org

Single-valuedness problem on charge density wave rings

T. HOSOKAWA[1], T. MATSUURA[1,2], M. TSUBOTA[3] and S. TANDA[1,2]

[1] *Department of Applied Physics, Hokkaido University - Sapporo 060-8628, Japan.*
[2] *Center of Education and Research for Topological Science and Technology, Hokkaido University Sapporo 060-8628, Japan*
[3] *Division of Quantum Science and Engineering, Hokkaido University - Sapporo 060-8628, Japan*

received 20 June 2015; accepted in final form 20 October 2015
published online 5 November 2015

PACS 71.45.Lr – Charge-density-wave systems
PACS 72.15.Nj – Collective modes (*e.g.*, in one-dimensional conductors)
PACS 03.65.Vf – Phases: geometric; dynamic or topological

Abstract – We investigate the bimodal fluctuation of charge density wave (CDW) current through ring-shaped crystals (typical diameter is a few ten μm) of orthorhombic tantalum trisulfide (o-TaS_3). We find that the CDW current changes between two types of the bimodal fluctuation, and exhibits hysteretic behavior as a function of the dc voltage. The hysteresis of the fluctuation modes suggests that the CDW rings involve several metastable sliding states, which might be a manifestation of single-valuedness of the CDW phase field with a strong periodic boundary condition of the ring geometry.

Introduction. – Single-valuedness of wave functions is a central role in physics on multi-connected spaces [1]. When a particle propagates around a closed ring, the wave function $\Psi(\theta)$ of the particle will interfere with itself, since $\Psi(\theta)$ is a single-valued function of position coordinate angle θ; $\Psi(\theta) = \Psi(\theta + 2\pi)$. A significant example is the Aharonov-Bohm effect for an electron propagating around a magnetic flux [2–4]. Macroscopic wave functions of condensed-matter phases, such as superfluid helium and superconductivity, also possess single-valuedness, and show quantized circulation of superfluid-helium persistent current, and quantized magnetic flux in superconducting rings, respectively.

Analogously, charge and spin density waves (CDW and SDW), degenerated macroscopic wave functions developed in low-dimensional electron systems [5], are expressed as a function of position x, such as $\rho_{\mathrm{CDW/SDW}}(x) = \rho_0 \cos(Q_{\mathrm{CDW/SDW}}x + \phi(x))$. However, the single-valuedness problem of CDW and SDW has never been studied explicitly.

Recent progress on synthesizing seamless ring-shaped single crystals of one-dimensional CDW materials with a diameter of a few ten micrometers opened a way for experimental investigation of CDWs in multi-connected space [6–10]. Tsubota *et al.*, revealed quantum behavior of CDW phase field dynamics using an Aharonov-Bohm quantum interference experiment with orthorhombic tantalum trisulfide (o-TaS_3) rings [11,12]. The authors found that a magnetoresistance oscillation with $\phi_0 = h/2e$, which might be the quantum interference of a CDW 2π phase soliton. Furthermore, they found that the CDW sliding current fluctuates temporally between two discrete values simultaneously with the magnetoresistance oscillation. The current switching behavior was clearly observed when a dc voltage 1.6 times larger than the threshold voltage of the CDW sliding was applied, while the previously observed current switching in $NbSe_3$ [13–17], $K_{0.30}MoO_3$ [18], and o-TaS_3 [19] whiskers had been observed only in the vicinity of the threshold voltage. These results suggested that a discrete CDW dynamics would be enhanced by the ring geometry.

In this manuscript, we report the effect on the single-valued function of CDWs revealed by the observation of the voltage hysteresis of CDW current fluctuation through ring-shaped o-TaS_3 crystals. At the CDW sliding regime, the CDW current shows bimodal fluctuation. Furthermore, the bimodal fluctuation has two kinds of switching modes [20]. An effect of the single-valuedness of CDW rings predicts four metastable states, which would correspond to each current state.

Experimental. – The ring-shaped o-TaS_3 crystals were synthesized by the chemical vapor transport method [11,12]. Tantalum wires and sulfur powder were

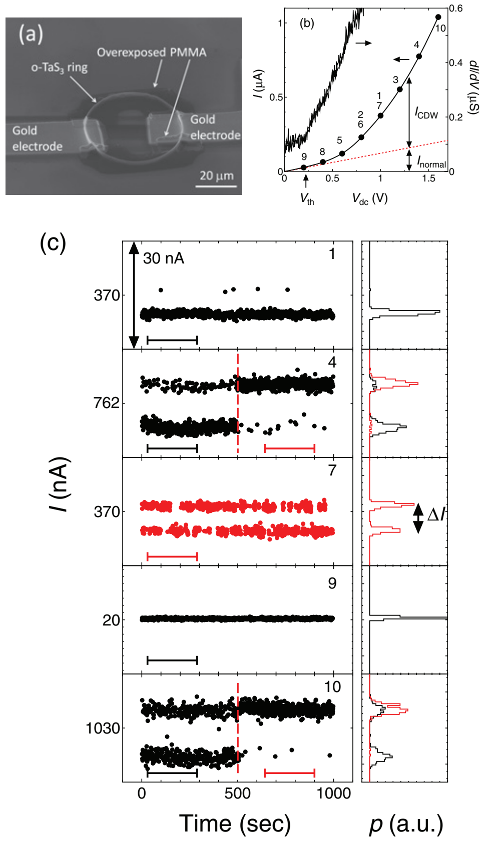

Fig. 1: (Color online) (a) Scanning electron microscopy image of a 45 μm diameter ring-shaped o-TaS_3 crystal, which is fixed on the substrate with overexposed PMMA films, and is attached to two gold electrodes using the electron beam lithography technique. (b) Current-voltage characteristic of the ring-shaped o-TaS_3 crystal at 80 K. The threshold voltage $V_{\rm th}$ is 0.2 V. The red broken line is the regression line of the Ohmic regime, which corresponds to the normal current of thermally excited electrons. The numbers on the curve indicate the order of the current fluctuation measurement. (c) Left panels: current fluctuation as a function of time for measurement 1, 4, 7, 9, and 10. A change of a switching mode is observed in measurement 4 and 10 at the moment indicated by the vertical red broken lines. The range of the vertical axis is 30 nA for all panels. Right panels: normalized probability distribution p of the measured current values. The colors of the distribution curves correspond to those of the time ranges indicated in the left panels.

heated for 3 hours in an evacuated quartz tube with a temperature gradient of 500 to 600 °C. Several ring-shaped crystals were found in fluff of o-TaS_3 whisker crystals. We picked each ring up and put it on an insulating SiO_2 substrate. Two gold electrical contacts were fabricated on the ring using an electron beam lithography technique.

The main data reported in this manuscript were obtained with the ring-shaped crystal shown in fig. 1(a). The crystal had a diameter of 45 μm, a radial thickness of 0.05 μm, and a width of 2.9 μm. Previous studies of the residual stress in ring-shaped crystals reported that no crystal dislocation is introduced for stress relaxation when the radial thickness of the ring-shaped crystals is less than $\sim 1\,\mu$m [21–24]. Therefore, thin ring-shaped crystals have as good a crystal quality as whisker crystals, and no CDW phase disorder is induced along the radial direction [9]. The nesting vector along the one-dimensional axis c is $Q_{\rm CDW} = 1/4c*$ at $T < 100$ K [25,26].

The room temperature resistivity is estimated to be $6 \times 10^{-6}\,\Omega$m, where the ring is treated as a parallel circuit. The CDW transition is observed at 220 K. No hysteresis of the low-field resistance is visible between the cooling and heating processes. The room temperature resistivity and the CDW transition temperature are consistent with the previous reported values for o-TaS_3 whisker crystals [27].

Results. – Figure 1(b) shows the dc voltage dependence of the dc current through the ring-shaped crystal at 80 K. The nonlinear conduction caused by the CDW sliding is observed above the threshold voltage ($V_{\rm th} = 0.2$ V). At the same temperature, we measure the current fluctuation of the CDW current at several constant dc voltages indicated by the filled circles. The numbers show the order of the temporal fluctuation measurement. The measurement starts at $V_{\rm dc} = 1$ V, which is in the sliding regime. Then the dc voltage is changed to $0.8, 1.2, 1.4\,\mathrm{V} \cdots$. The current value is measured with a picoammeter (Keithley) every second, and a total of 50000 measurement points are obtained for each constant dc voltage.

The current fluctuations for several dc voltages over a period of 1000 seconds selected from all the measurement points are shown in the left panels of fig. 1(c). The right panels show the normalized probability distributions of the current values. In measurement 1 ($V_{\rm dc} = 1$ V), we observe that the current temporally switches between the lower and the higher values. The bimodal fluctuation is consistent with that reported in a previous work [12]. This discretization is not caused by the minimum digit of the picoammeter or accuracy of the measurement system. Note that we have observed no clear magnetic-field dependence in the switching phenomena in this ring-shaped crystal. The reason for this remains unclear. Here we focus on the dc voltage dependence of the temporal current switching.

In measurement 1–4, when the dc voltage is increased, current difference between the lower and higher current (ΔI) and one-state fluctuation are increased. There is a tendency for the probability of the higher current to increase when the applied dc voltage increases.

In measurement 4 ($V_{\rm dc} = 1.4$ V), after several hundred seconds from the measurement started, the switching mode changes at the moment indicated by the red broken line in the second panel on the left in fig. 1(c). The change of the switching mode is clearly seen also in the probability distributions shown in the right panel. In the black probability distribution is that for before the mode change, and the lower current state is predominant. After the mode change, the probability of the higher current state changes that drawn in red. Hereafter, we call the first and second

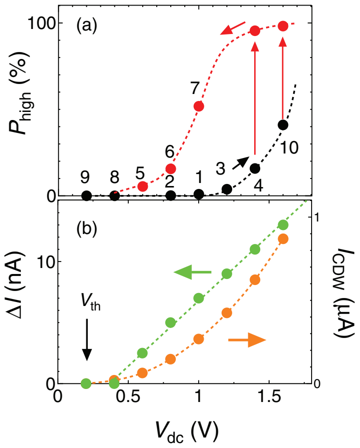

Fig. 2: (Color online) (a) Hysteretic behavior of probability at the higher current state as a function of the CDW current. The numbers on the circles correspond to the order numbers in fig. 1(b). The vertical arrows show the change from the black trace (switching mode A) to the red trace (switching mode B). (b) Voltage dependence of the CDW current (blue filled circles) and the difference between the current values of the higher and lower current states (green filled circles). The broken curves are guides for the eye.

switching modes as "mode A" and "mode B", respectively, for convenience.

We find that the mode change is hysteretic. In measurements 5–7, the mode remains B even the dc voltage is reduced below 1.4 V. The result of measurements 7 is clearly different from that of measurements 1. When $I_{\rm CDW} = 0$ (in measurement 9), no switching behavior was observed ($\Delta I = 0$). After that time, we observed the change of the switching mode from A to B again at $V_{\rm dc} = 1.6$ V in measurement 10. The mode change is reproducible, and can be reset by reducing the dc voltage to below the threshold voltage. The hysteresis of the current switching mode was observed in NbS_3 rings at 100 K.

The probability at the higher current state $P_{\rm high} \equiv N_{\rm high}/(N_{\rm high} + N_{\rm low})$ is displayed in fig. 2(a) as a function of the dc voltage, where $N_{\rm high}$, and $N_{\rm low}$ are the number of data points recognized to higher and lower current states, respectively. In mode A, $P_{\rm high}$ follows the black trace. It appears that when the dc voltage exceeds 1.4 V, the switching mode can change easily from A to B. After the mode change, $P_{\rm high}$ follows the red trace. When $I_{\rm CDW} = 0$, the switching mode is reset to A, and then $P_{\rm high}$ again follows the black trace.

It seems that amplitude of fluctuation ΔI might have a physical meaning since it is conserved before and after the switching mode change. We plot ΔI as a function of the dc voltage in fig. 2(b). ΔI is a linear function of $V_{\rm dc}$, while the CDW current $I_{\rm CDW}$ is not inear with respect to the dc voltage. The results implies that the current fluctuation is caused by extra charge carrier, such as CDW phase solitons, but not fluctuation of conventional CDW sliding current.

Discussion. – The discrete probability distribution suggests that the CDW current fluctuates between many metastable states. Furthermore, there is several switching modes. For the bimodal fluctuation at 80 K, ΔI is conserved before and after the switching mode change. We plot ΔI as a function of the dc voltage in fig. 2(b). ΔI is a linear function of $V_{\rm dc}$, while the CDW current $I_{\rm CDW}$ is not linear with respect to the dc voltage. The results imply that the current fluctuation is caused by extra charge carriers, such as CDW phase solitons, but not fluctuation of conventional CDW sliding current.

The metastable states were considered to be caused by the CDW phase field modulation. As regards $NbSe_3$ [13–17], $K_{0.30}MoO_3$ [18], and o-TaS_3 [19] whiskers, impurities or electrical contacts act as strong pinning centers. Depending on the impurity positions, several metastable states of the CDW phase field will emerge. The current (or voltage) induced switching between two metastable states could be considered the origin of the electrical current switching. Such quantized behavior was also observed in Ohmic regime for small one-dimensional CDW materials of o-TaS_3, $NbSe_3$ and $K_{0.30}MoO_3$ [28–30]. The number of one CDW wavelength between the electrical contacts was quantized. We note that the X-ray observation of $Q_{\rm CDW}$ distribution in the sliding regime showed that observed phase slipping region modulated by applied electric field is over mm [31]. Thus our CDW rings are too small to exhibit the phase slipping phenomenon.

In the case of the ring-shaped crystals, the ring geometry would dominate the phase field modulation because the boundary condition restricts CDWs. A single-valued function of the CDW is imposed to ensure that $\rho_{\rm CDW}(x) = \rho_{\rm CDW}(x + 2\pi R)$, where R is radius of the ring. The phase factor of the CDW is required the following condition:

$$\oint_C \partial_x \left(Q_{\rm CDW} x + \phi(x)\right) \cdot {\rm d}x = 2\pi n_{\rm CDW}, \tag{1}$$

where x is coordinate on the ring of the one-dimensional chain C. $n_{\rm CDW}$ is an integer number. Equation (1) is a strong boundary condition for $\phi(x)$. In the real CDW rings, the extra phase $\phi(x)$ must be finite, except $Q_{\rm CDW} R =$ an integer number. Therefore, the ring-shaped crystals at a CDW state become electrically charged, since $\partial\phi/\partial x$ is proportional to extra electron desnity. An extra charge in a CDW ring is analogous with a magnetic flux penetrating a superconducting ring.

There are two possible ways for finite $\phi(x)$. The first one is homogeneous phase modulation, and the second one is generation of CDW phase solitons, as shown in fig. 3. A homogeneous phase modulation changes the CDW wavelength. On the other hand, the CDW rings can make a fractional/irrational phase soliton. The electrical charge and phase difference of a soliton must be less than $2e$ and 2π. Such solitons should be localized across the whole cross-section and become a soliton wall, due to the interchain coupling energy. The fractional/irrational soliton

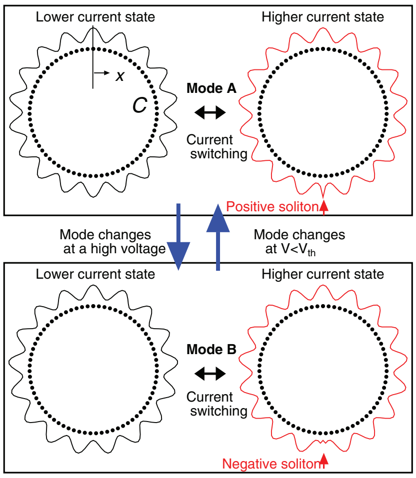

Fig. 3: (Color online) Schematics of one-dimensional CDWs of $Q_{\mathrm{CDW}}R = 17.5$ at lower and higher current states, respectively. Black dots indicate crystal lattice. The upper panel shows current switching between the CDW ring of $Q_{\mathrm{CDW}}R = 18$ and that of $Q_{\mathrm{CDW}}R = 17.5$ with a positive half (π) phase soliton. The lower panel shows current switching between the CDW ring of $Q_{\mathrm{CDW}}R = 17$ and that of $Q_{\mathrm{CDW}}R = 17.5$ with a negative half ($-\pi$) phase soliton.

is different from the 2π solitons [32–34] or the amplitude solitons [35] that can exist individually.

The fractional/irrational phase soliton can explain the experimental results that $\Delta I/I_{\mathrm{CDW}} \sim 10^{-3}$. The soliton wall of the fractional/irrational phase solitons carries a large number of electrical charges. If the soliton mobility would greatly exceed the CDW sliding, the conductivity increases. Thus the soliton state could be the higher current state of the current switching. On the other hand, the homogeneous modulation of CDW wavelength is just a small change for the sliding current, since a modulation of Q_{CDW} would be roughly of the order of 10^{-5} for a ring-shaped crystal with a 45 μm diameter. The small change of Q_{CDW} does not lead a large change of the sliding current. Moreover, if the extra charge might be induced uncondensed electrons/holes, the effect of them in the Ohmic conduction is just the order of $10^{-4} - 10^{-5}$ [28–30]. Therefore, both of the effects in the homogeneous modulation could not make an effective change in the CDW current. Thus the homogeneous modulation is regarded as the lower current state. The CDW fluctuate the homogeneous modulation state and the fractional/irrational soliton state with an assistance of electrical current at the sliding regime, while n_{CDW} is conserved.

The mode change could be regarded as switching between the negatively charged states ($n_{\mathrm{CDW}} > Q_{\mathrm{CDW}}R$) and positively charged states ($n_{\mathrm{CDW}} < Q_{\mathrm{CDW}}R$), as shown in the upper and lower panels in fig. 3. The negative fractional/irrational soliton carries electrical charge that moves to the opposite direction of the sliding CDW. The lowest four energy metastable states can realize. The fluctuation between the homogeneous modulation state and the soliton states are current switching. The hysteretic change between the negatively charged states and the positively charged states could correspond to the mode change between A and B. The free energies of the four metastable states will differ depending on the value of $Q_{\mathrm{CDW}}R$ for each ring-shaped crystal. Then the probability distribution of modes A and B will be different.

Summary. – We demonstrated the dc voltage hysteresis of the CDW current switching probability in o-TaS_3 ring-shaped crystals. We discussed that the hysteresis is caused by the effect of single-valuedness for the CDW rings. The previous experiments of the Aharonov-Bohm magnetoresistance oscillation suggest the single-valuedness of the quantum wave function of phase solitons, but the coupling mechanism between the current switching is unclear yet [12]. To solve this problem, a CDW might be treated as a quantum wave function within the framework of the Ginzburg-Landau theory [36].

* * *

We thank T. Tsuneta, N. Matsunaga, K. Yamaya, K. Nakatsugawa, K. Yamaguchi, K. Katono and K. Ichimura, for fruitful discussions and experimental support. This work is supported by Iketani Science and Technology Foundation 0241040-A, Hitachi Metals · Materials Science Foundation, and the JSPS KAKENHI Grant Nos. 12837528, and 26287069.

REFERENCES

[1] Merzbacher E., *Am. J. Phys.*, **30** (1962) 237.
[2] Aharonov Y. and Bohm D., *Phys. Rev.*, **115** (1959) 485.
[3] Ehrenberg W. and Siday R. E., *Proc. Phys. Soc. B*, **62** (1949) 8.
[4] Tonomura A., Matsuda T., Suzuki R., Fukuhara A., Osakabe N., Umezaki H., Endo J., Shinagawa K., Sugita Y. and Fujiwara H., *Phys. Rev. Lett.*, **48** (1982) 1443.
[5] Monceau P., *Adv. Phys.*, **61** (2012) 325.
[6] Tanda S., Tsuneta M., Okajima Y., Inagaki K., Yamaya K. and Hatakenaka N., *Nature*, **417** (2001) 397.
[7] Tsuneta T. and Tanda S., *J. Cryst. Growth*, **264** (2004) 223.
[8] Matsuura T., Tsuneta T., Inagaki K. and Tanda S., *Phys. Rev. B*, **73** (2006) 165118.
[9] Shimatake K., Toda Y. and Tanda S., *Phys. Rev. B*, **73** (2006) 153403.
[10] Matsuura T., Inagaki K. and Tanda S., *Phys. Rev. B*, **79** (2009) 014304.
[11] Tsubota M., Inagaki K. and Tanda S., *Physica B*, **404** (2009) 416.
[12] Tsubota M., Inagaki K., Matsuura T. and Tanda S., *EPL*, **97** (2012) 57011.
[13] Zettl A. and Grüner G., *Phys. Rev. B*, **26** (1982) 2298.
[14] Bloom I., Marley A. C. and Weissman M. B., *Phys. Rev. B*, **50** (1994) 5081.

[15] Hall R. P., Hundley M. F. and Zettl A., *Phys. Rev. B*, **38** (1988) 13002.

[16] Hall R. P. and Zettl A., *Phys. Rev. B*, **38** (1988) 13019.

[17] Sherwin M. S., Zettl A. and Hall R. P., *Phys. Rev. B*, **38** (1988) 13028.

[18] Dumas J., Schlenker C., Marcus J. and Buder R., *Phys. Rev. Lett.*, **50** (1983) 757.

[19] Mihály L. and Grüner G., *Solid State Commun.*, **50** (1984) 807.

[20] Hosokawa T., Matsuura T., Tsubota M. and Tanda S., *Physica B*, **460** (2015) 171.

[21] Hayashi M., Ebisawa H. and Kuboki K., *Europhys. Lett.*, **76** (2006) 264.

[22] Tsuneta T., Yamamoto K., Ikeda N., Nogami Y., Matsuura T. and Tanda S., *Phys. Rev. B*, **82** (2010) 014105.

[23] Matsuura T., Tsuneta T., Kumagai G., Tsubota M., Matsuyama T. and Tanda S., *Phys. Rev. B*, **83** (2011) 174113.

[24] Tsubota M., Inagaki K., Matsuura T. and Tanda S., *Cryst. Growth Design*, **11** (2011) 4789.

[25] Roucau C., Ayroles R., Monceau P., Guemas L., Mefrschaut A. and Rouxel J., *Phys. Status Solidi (a)*, **62** (1980) 483.

[26] Inagaki K., Tsubota M., Higashiyama K., Ichimura K., Tanda S., Yamamoto K., Hanasaki N., Ikeda N., Nogami Y., Ito T. and Toyokawa H., *J. Phys. Soc. Jpn.*, **77** (2008) 093708.

[27] Thompson A. H., Zettl A. and Grüner G., *Phys. Rev. Lett.*, **47** (1981) 64.

[28] Zybtsev S. V., Prokrovskii V. Ya. and Zaitsev-Sotov S. V., *Nat. Commun.*, **1** (2010) 85.

[29] Zybtsev S. V. and Prokrovskii V. Ya., *Phys. Rev. B*, **84** (2011) 085139.

[30] Borodin D. V., Zaitsev-Zotov S. V. and Nad' F. Ya., *Zh. Eksp. Teor. Fiz.*, **93** (1987) 1394.

[31] Rideau D., Monceau P., Currat R., Requardt H., Nad F., Lorenzo J. E., Brazovskii S., Detlefs C. and Grübel G., *Europhys. Lett.*, **56** (2001) 289.

[32] Miller J. H., Wijesinghe A. I., Tang Z. and Guloy A. M., *Phys. Rev. Lett.*, **108** (2012) 036404.

[33] Miller J. H. jr., Wijesinghe A. I., Tang Z. and Guloy A. M., *Phys. Rev. B*, **87** (2013) 115127.

[34] Matsuura T., Hara J., Inagaki K., Tsubota M., Hosokawa T. and Tanda S., *EPL*, **109** (2015) 27005.

[35] Brazovskii S., Brun C., Wang Z. Z. and Monceau P., *Phys. Rev. Lett.*, **108** (2012) 096801.

[36] Tütto I. and Zawadowski A., *Phys. Rev. B*, **32** (1985) 2449.